Group 7 | Tabiscope: Mobile Device Camera Connector
Daniel Ahn

Partners: Deepak Lingam, Kyle Wong
Mentors: Dr. Amit Kochhar, Dr. Simon Best, Kevin Olds

Stehle, Thomas. "Removal of specular reflections in endoscopic images." *Acta Polytechnica* 46.4 (2006).
Kaup, André, Katrin Meisinger, and Til Aach. "Frequency selective signal extrapolation with applications to error concealment in image communication." *AEU-International Journal of Electronics and Communications* 59.3 (2005): 147-156.

Project Goal and Relevance

The goal of this project is to provide a low-cost alternative to the traditional endoscopic image systems that are expensive and not portable. There are already existing solutions such as Endoscope-I that consist of an imaging software and an endoscope adapter to iPhone. Clinicians who used it, however, pointed out some limitations of this existing solution. Firstly, they complained that Endoscope-I's resolution is limited to small screen size of iPhone. To address this issue, our group chose to use an Android tablet for bigger screen size. Secondly, its image quality is not as good as traditional imaging towers'. We suspect that it is because Endoscope-I's iPhone application uses iPhone's existing internal camera application and there is no image processing, whereas traditional imaging towers usually have image processing processors. Therefore, a camera application with low control and real-time image process algorithm need to be implemented on the tablet to address these issues.

Since a tablet has stronger computational power than an iPhone, some real-time image processing can be done to improve the image quality. For example, using Randomized Hough Transformation (RHT), an algorithm can be implemented for a tablet automatically to detect the region of interest, usually a circular shape, and for the tablet to focus on this area. More specifically, among many issues with image quality, clinicians pointed out that the specular reflection phenomena occurs more often in iPhones than it does in the towers. This issue might get resolved by implementing image processing algorithm for removing specular reflection. Although there is no known perfect algorithm that can remove specular reflection from image, we review these two papers, Stehle (2006) and Kaup et al. (2005), in order to assess whether it is feasible to provide a software-based solution to the existing issues with specular reflection.

Motivation

Stehle wrote this paper in order to address specular reflection issues in *PillCam*, which is used for gastointestinal tract imaging by having patients swallowing this wireless camera. Since with PillCam it is impossible for clinicians to adjust direction of endoscopic camera to lessen the effect of specular reflection, he proposes an algorithm that can remove the reflection by deleting the reflective region and interpolating the region with surrounding region's information, as it is shown in Figure 1. The idea of segmenting reflective region by luminance already existed prior to his work. Stehle's implementation is novel in providing a way of correcting the segmented region. He calls the correcting algorithm "defect interpolation", as it is shown in Figure 1. Interestingly, much of this comes from more theoretical paper, Kaup et al. (2005), where the

works were created under very different motivation. They proposed a method to conceal error in video communication and additionally to eliminate defective pixels in X-ray imaging.
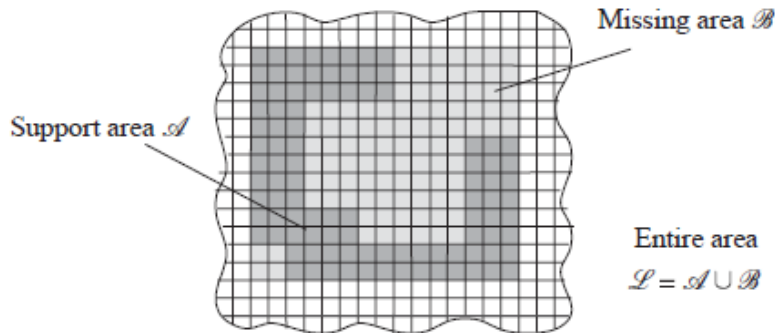

Figure 1 The principle of extrapolation: the missing area B (light gray) is extrapolated from the approximated support area (dark gray); Adapted from Kaup et al. (2005)
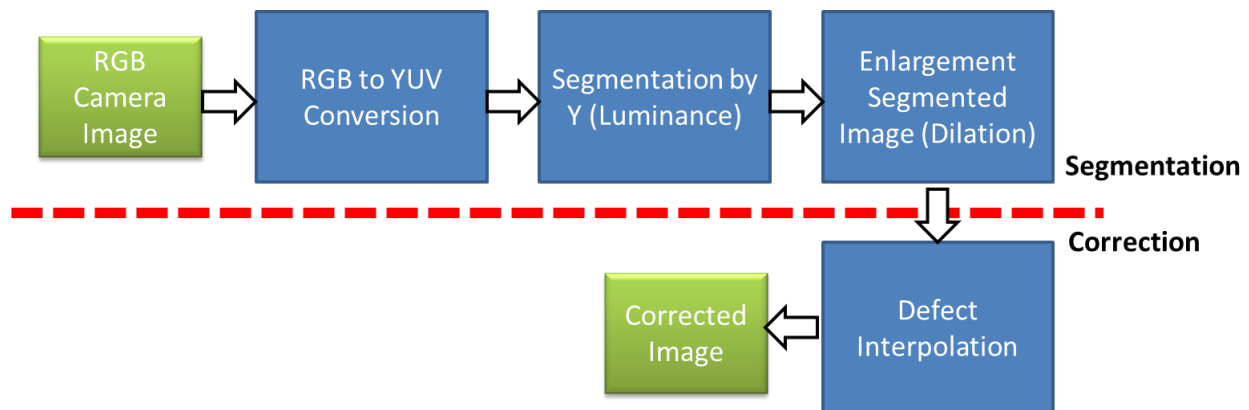

Figure 2 Stehle (2006) Specular Reflection Algorithm Overview

Method

Stehle (2006)'s algorithm can be understood in two parts: segmentation of defective (reflective) pixel and removal of this pixel as it is shown in Figure 2.

1. Segmentation

Segmentation method can be classified as 3-steps process. This process is computationally and algorithmically trivial.

1.1 *RGB to YUV Conversion*

Equation 1 RGB to YUV conversion

$$\begin{bmatrix} Y \\ U \\ V \end{bmatrix} = \begin{bmatrix} 0.299 & 0.587 & 0.114 \\ -0.147 & -0.289 & 0.436 \\ 0.615 & -0.515 & -0.100 \end{bmatrix} \cdot \begin{bmatrix} R \\ G \\ B \end{bmatrix}$$

Using Equation 1, image can be converted from RGB color space to YUV space. By doing this, we can easily obtain pixels' luminance in YUV space, which correlates with reflectiveness of pixels.
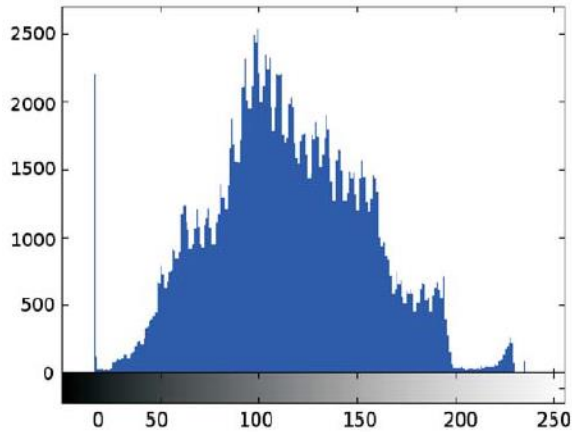
1.2 *Segmentation by Y*

Figure 3 Histogram of the luminance channel of an endoscopic image containing specular reflections; Adapted from Figure 1 of Stehle (2006)

In Figure 3, the small peak on the right corresponds to pixels that contain specular reflections. Using the cut off value of luminance between this peak and the rest, the whole image can be segmented as 1 if it is normal pixel, 0 if it is defective pixel with specular reflection.

1.3 *Dilation of Segmented Image*

The segmented image is dilated in order to enlarge the segmentation. For the experiment, Stehle used 9x9 circular structure.

2. Defect Interpolation: Iterative Spectral Deconvolution

Mathematical approach of this step is adapted from Kaup et al. (2005). Stehle applied 100 iterations of the Deconvolution algorithm. The illustration of the recursive spectral deconvolution algorithm can be found in Figure 4.

He defines $g(n)$ as observed image, note here that the notation is written as if the signal is 1D for simplification. $f(n)$ denotes the undisturbed image and $w(n)$ denotes a binary window with $w(n) = 0$ if the corresponding pixel n in $g(n)$ belongs to a reflection and $w(n) = 1$, otherwise. $G(k), F(k)$, and $W(k)$ are the DFT spectra of $g(n)$, $f(n)$, and w(n), respectively.

The goal of this algorithm is to estimate the discrete Fourier transformation between $F(k)$ and $f(n)$. It is done by iteratively improving a spectral line pair, or *line spectrum pair* (LSP). He also uses $\hat{F}(k)$, $\widehat{F^*}(k)$ to represent the estimated spectral coefficient. Note that $\widehat{F^*}(k) = \hat{F}(N - k)$.

If we select a spectral line pair $G(s)$ and $G(N - s)$ and $F(k)$ consists only of two lines at s and N-s, then

$$F(k) = \hat{F}(k) = \hat{F}(s)\delta(k - s) + \hat{F}(N - s)\delta(k - N + s)$$

and $F(k)$ convolution with $W(k)$ would yield

$$G(s) = \frac{1}{N}\left(\hat{F}(s) \cdot W(0) + \hat{F}^*(s) \cdot W(2s)\right)$$

$$G^*(s) = \frac{1}{N}\left(\hat{F}^*(s) \cdot W^*(0) + \hat{F}(s) \cdot W^*(2s)\right),$$

.

From this, $\hat{F}(s)$ can be found.

$$\hat{F}(s) = N \frac{G(s)W(0) - G^*(s)W(2s)}{|W(0)|^2 - |W(2s)|^2}.$$

Generally, F(k) consist of more than two spectral lines. Now we can find error after deconvolution at s and N-s in the spectral domain, given by

$$G^{(1)}(k) = G(k) - \frac{1}{N} \cdot \hat{F}(k) * W(k)$$

$$= G(k) - \frac{1}{N}\left(\hat{F}(s) \cdot W(k-s) + \hat{F}^*(s) \cdot W(k+s)\right).$$

If the selected line G(s) and G($N - s$) is dominant, its convolution with W(k) tends to "hide" other less dominant spectral coefficient of F(k). This leads to the following iteration for spectral deconvolution.

- Initialization

$$\hat{F}^{(0)}(k) = 0,\, G^{(0)}(k) = G(k),\, i = 1.$$

- i-th iteration step:

Select a pair of coefficients

$$G^{(i-1)}(s^{(i)}),\, G^{(i-1)}(N - s^{(i)}) \text{ out of } G^{(i-1)}(k).$$

- Estimate $\hat{F}(s^{(i)}), \hat{F}(N - s^{(i)})$

$$G^{(i-1)}(s^{(i)}) = \frac{1}{N}\left(\hat{F}(s^{(i)})W(0) + \hat{F}^*(s^{(i)})W(2s^{(i)})\right)$$

$$G^{*(i-1)}(s^{(i)}) = \frac{1}{N}\left(\hat{F}^*(s^{(i)})W(0) + \hat{F}(s^{(i)})W^*(2s^{(i)})\right)$$

$$\Rightarrow$$

$$\hat{F}(s^{(i)}) =$$

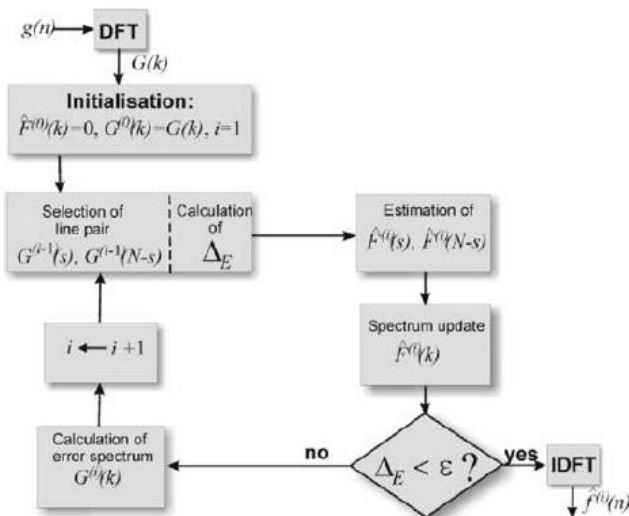$$N \frac{G^{(i-1)}(s^{(i)})W(0) - \left(G^{(i-1)}(s^{(i)})\right)^* W(2s^{(i)})}{|W(0)|^2 - |W(2s^{(i)})|^2}.$$

Figure 4 Iterative Spectral Deconvolution Algorithm; Adapted from Figure 2 of Stehle (2006)
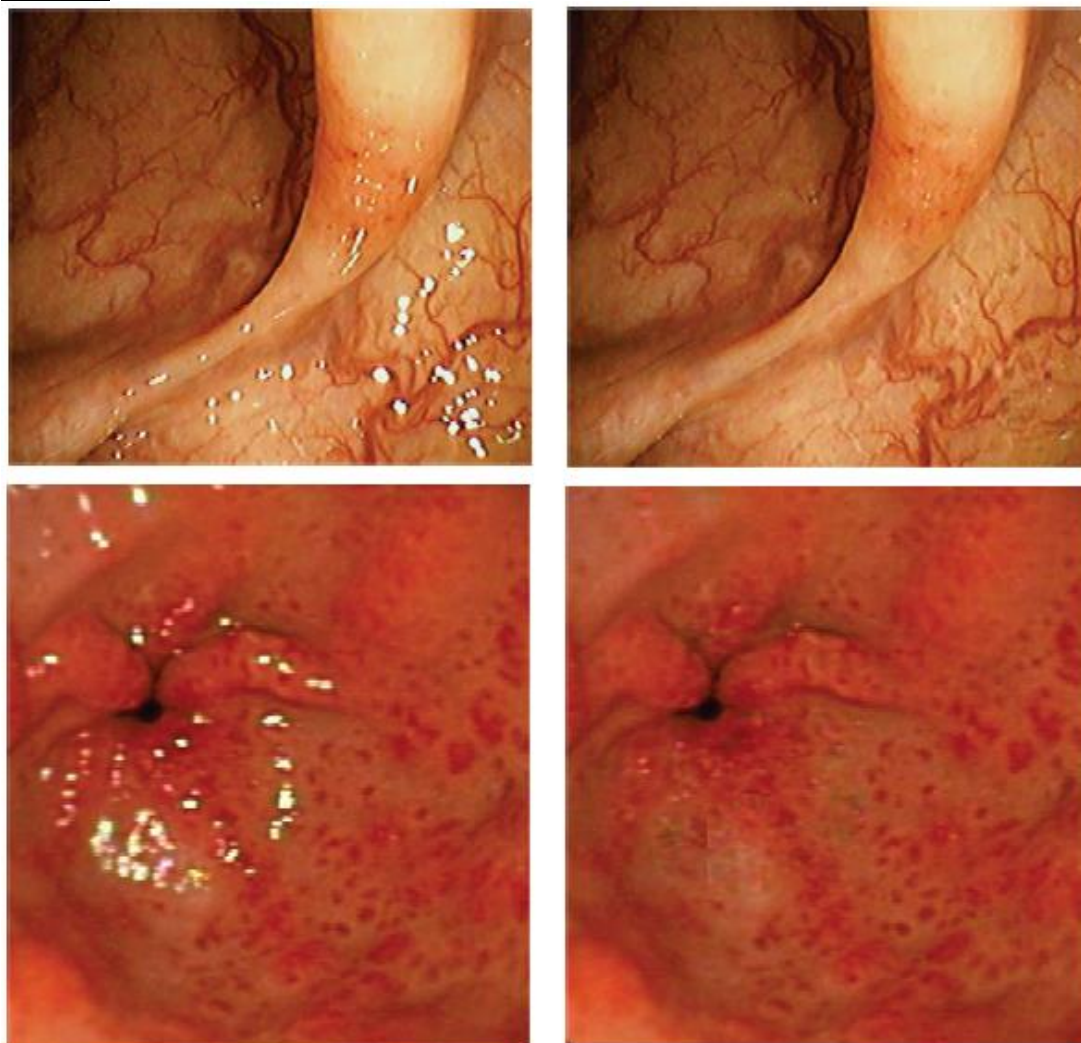
Result

Figure 5 Adapted from Figure 3 and Figure 4 of Stehle (2006); Endoscopic image of the colon with specular reflections (top left) and processed image (top right). The overall impression of the processed image is better, but some artifacts have been added to the image. The vessels in the lower right corner appear blurred, and some of them interrupted. Similarly endoscopic image of the esophagus with specular reflections (bottom left) and the processed image (bottom right). In areas with a large number of specular reflections block artifacts have been added to the image.

As it is shown in Figure 5, the entire workflow described in the previous section was used to generate corrected images from images corrupted by specular reflection. It is shown from the image that overall specular reflection is removed. However, there are some remaining artifacts. In top right corner, we can find that some of vessels appeared interrupted. In bottom right corner, we can also find that block artifacts were added to image in areas where a large number of specular reflections occurred.

In the original spectral deconvolution paper, however, as shown in Figure 6, error containing block is concealed pretty uniformly without many aritifacts.

Figure 6 Concealment of block losses using the frequency selective extrapolation technique. Left: Isolated 16 × 16 block losses. Right: Concealed image; Adapted from Figure 5 of Kaup et al. (2005)

Assessment and Concluding Remark

1. Stehle (2006)

- Experiment was not performed on video

Since experiment was not performed on a video, it is not clear how well it will work with a video frames where each frame is not well focused as still picture.

- Lack of numerical, quantitative evaluation

Stehle only concluded his paper with qualitative evaluation.

- Lack of feedback from clinicians

Stehle states that "processed images have not been presented to a physician because of the drawbacks…" The quality of image was never assessed by clinicians.

- Running time

Although Stehle did not specify which platform he was using, since it requires recursive iteration and some expensive computation on discrete Fourier transformation, tablet might not be suitable to produce on-the-fly specular-reflection-corrected image.

Stehle (2006) made an interesting application of the error concealment algorithm developed in the field of image communication. However, the algorithm is not yet refined enough so it is not suitable for our application because it is not fast enough for on-the-fly application. Also, the image quality is never assessed by clinicians and it seems to be a large drawback because it removes or blurs out important details from image such as blood vessels.

For our purpose it might be more efficient to implement a device to control the light source when specular reflection is detected.